

# A new representation of the bulk current in the quantum Hall effect regime

Josef Oswald

*Institute of Physics, University of Leoben, Franz Josef Str.18,  
A-8700 Leoben, Austria, e-mail: josef.oswald@unileoben.ac.at*

(Dated: November 14, 2018)

In preceding papers a Landauer-Büttiker type representation of bulk current transport has been successfully used for the numerical simulation of the magneto transport of 2-dimensional electron systems in the high magnetic field regime. In this paper it is demonstrated, that this representation is in full agreement with a treatment of the bulk current transport as a tunneling process between magnetic bound states. Additionally we find a correspondence between our network representation and the bulk current picture in terms of mixed phases mapped on a checkerboard: At half filled Landau level (LL) coupled droplets of a quantum Hall (QH) liquid phase and coupled droplets of an insulator phase exist at the same time, with each of them occupying half of the sample area. Removing a single electron from to such a QH liquid droplet at half filling completes the QH transition to the next higher QH plateau. Adding a single electron to such a droplet at half filling completes the QH transition to the previous lower QH plateau. As a consequence, the sharpness of the QH plateau transitions on the magnetic field axis depends on the typical size of the droplets, which can be understood as a measure of the disorder in the sample.

PACS numbers: 73.43.-f, 73.40.Gk, 73.43.Nq, 73.43.Qt

## I. INTRODUCTION

Even more than 20 years after the discovery of the integer quantum Hall effect there are still controversial discussions about the origin of this phenomenon. In particular the transition regime between plateaus gained increasing attention during the last two decades. While it is commonly accepted, that the plateau values of the integer quantum Hall effect (IQHE) can be explained by the edge channel (EC) picture[1, 2, 3, 4], the transition regime between plateaus is believed to be driven by a different mechanism in the bulk of the sample. A well defined scaling behavior of the temperature dependence is seen as an evidence for a quantum phase transition in the vicinity of the QHE plateau transitions [5, 6, 7, 8, 9] (for a review see also Refs. [10, 11]). While the existence of a formal equivalence of the edge channel picture and the bulk current picture is proposed by Ruzin et al.[12], the investigations of non-equilibrium situations like selective edge channel population, AC-characteristics and non-linear transport give evidence, that edge channels should be more than just a different representation of bulk currents. Since more than two decades the fundamental question concerning edge vs. bulk in the QHE gets permanent attention even until now, as can be seen from a representative selection of references: Starting with the discovery of the IQHE [13] and first systematic experiments investigating different contact configurations [14, 15], continuing with the introduction of edge channels by Büttiker [1] and the enormous number of examples for dealing with the edge vs. bulk problem and making use of the EC picture for modeling and interpretation of experiments [16, 17, 18, 19, 20, 21, 22, 23, 24, 25, 26, 27, 28, 29, 30, 31, 32, 33, 34, 35, 36, 37, 38, 39, 40, 41, 42, 43, 44, 45, 46, 47, 48, 49, 50, 51, 52, 53, 54, 55, 56, 57, 58, 59, 60, 61, 62, 63, 64, 65, 66,

67, 68, 69, 70, 71, 72, 73, 74, 75, 76, 77, 78, 79, 80, 81, 82, 83, 84, 85, 86, 87, 88, 89, 90, 91], still a remarkable number of most recent papers on this topic can be found [92, 93, 94, 95, 96, 97, 98, 99, 100, 101, 102, 103, 104, 105, 106, 107, 108, 109, 110]. Concerning experimental probing of edge channels, major improvements of the experimental techniques have been achieved in the last few years [37, 44, 48, 52, 78, 80, 81, 82, 83, 88, 89, 110]. A very fundamental aspect of edge channels is the drastic enhancement of the phase coherence length of electrons within edge states. Major work on this topic has been done by Komiyama et al [93].

Concerning modeling of quantum transport, one of the very first attempts can be attributed to R.Landauer[111, 112]. A major step forward was achieved by M. Büttiker by introducing the so-called Landauer-Büttiker (LB) formalism and the EC-picture of the QHE[1]. For modeling quantum transport and localization in the bulk, mainly network models on the basis of the Chalker Coddington (CC) network [113] are used. However, a model, which generates data in terms of voltages and resistances, which would allow a direct comparison which experimental data for realistically shaped samples had not been developed so far. In order to do so, an approach to combine EC transport and bulk transport has been made some time ago [68, 71]. Subsequently that model has been expanded to a network[85], which is also the subject of this paper. Although the basic idea of our network is common with the basic idea of the CC network, our handling of the nodes is substantially different: In contrast to a CC network our network does not use a transfer matrix for amplitudes and phases. We use transmission by tunneling, but incorporating the effect of tunneling according to the LB formalism. The nodes are described by a back scattering function  $P$ , which is the ration of reflection and transmission coefficient  $R/T$ .

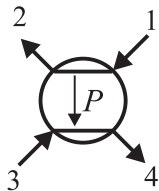


FIG. 1: Node of the network with two incoming and two outgoing channels. The channels  $1 \rightarrow 2$  and  $3 \rightarrow 4$  are treated like edge channels with back scattering, where  $P = R/T$  according to the Landauer- Büttiker formalism.

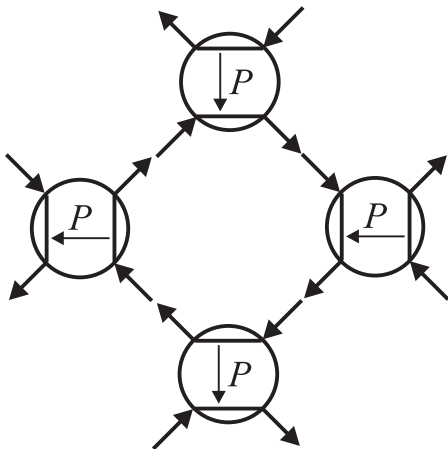


FIG. 2: Arrangement of the nodes for building the minimal physical element of a network, which is the closed loop of a so called magnetic bound state (see below)

In Fig.1 a single node of the network is shown, which transmits potentials from the incoming to the outgoing channels. The transmitted potentials of the outgoing channels as a function of  $P$  is calculated as follows [85]:

$$\mu_2 = (\mu_1 + P \cdot \mu_3)/(1 + P) \quad (1a)$$

$$\mu_4 = (\mu_4 + P \cdot \mu_1)/(1 + P) \quad (1b)$$

In Fig.2 it is shown, how a network is build by arranging the nodes. The minimum network forms a loop, which corresponds physically to a single magnetic bound state. A periodic continuation of this network leads to further adjacent loops, which get coupled by the nodes. In this way the network transmits potentials and the potential distribution is calculated by an appropriate iteration procedure. Currents are obtained only after obtaining the solution for the potential distribution within the whole network. Because of using just reflection and transmission coefficients so far, phase coherence between adjacent loops is not explicitly included. Despite this fact, this network allows to simulate IQHE experiments with realistic sample geometry in almost all details[85, 90]. The key-point of this approach is the

representation of the back scattering function  $P$ , which will be considered in more detail in the main part of this paper.

Considering the nodes of the network, they can be understood as elementary QH - samples with a single EC pair experiencing back scattering, which is described by the function  $P$ . Originally this function had been used as representative for a QHE sample as a whole and it had to be defined for each LL separately as  $P = P(\Delta\nu)$ [68, 71].  $\Delta\nu$  is the filling factor of the corresponding LL relative to half filling. The total sample behavior was obtained by summing up the components of the conductance tensor of all LLs. In [71] it had been shown, that in order to meet all symmetry relations found in experimental data [62, 67],  $P(\Delta\nu)$  has to be an exponential function  $P(\Delta\nu) = \exp(-\Delta\nu/k)$ . On this background this function has to be seen as a semi-empirical function so far. Nevertheless, just assuming the existence of this function allowed to explain already quite a number of universal features of the IQHE without referring to a special choice of the pre-factor  $k$  in the exponent. The function  $P(\Delta\nu)$  also allows to obtain a scaling behavior by considering the factor  $k$  as a temperature dependent function  $k(T)$ . In [71] it has been shown, that any not necessarily known function  $k(T)$  is mapped out directly by the temperature scaling function for  $R_{xx}$  and  $R_{xy}$ .

The basic idea, which subsequently led to the usage of  $P(\Delta\nu)$  also within a network approach, is that current transport at high magnetic fields in the bulk region may happen via tunneling between magnetic bound states. Such bound states are considered to be physically equivalent to ECs. Thus, these bound states are closed loops of directed channels and are created in real samples by smooth potential fluctuations at high magnetic fields. Tunneling between such loops happens preferably near the saddle points of the random potential. The most important ingredient of our network is that the tunneling current can be handled as a back scattering process in the EC-picture like already outlined above. This makes our network approach essential different from the Chalker-Coddington model[113] and all network approaches derived from this[115, 116, 117]. Just to clarify, the CC network maintains coherence on the entire network, while the largest coherent element in our network is a single loop, which at the same time defines the size of a network period  $L$ . If we consider the in-elastic scattering length  $L_{in}$  of the electron system and the size of the sample  $L_p$ , then the CC network deals with the regime  $L < L_p \leq L_{in}$ , while our network considers the regime  $L_{in} \leq L < L_p$ . From this point of view our network does not necessarily contradict the CC-network, but addresses a different regime. As will be shown in this paper, the tunneling process is well represented by the back scattering function  $P(\Delta\nu)$  used in [85]. It can be calculated locally at the designated grid points from the magnetic field and the local carrier density. On this basis it is possible to model the shape the sample by shaping the lateral carrier distribution. By doing so, it has

been shown for the first time, that the influence of sample geometry (such as contact arms) and carrier density inhomogeneities (like introduced by gate electrodes) can be successfully addressed on the basis of a network model in full agreement with experimental results [85, 90]. While the main task of [85] was to present the technical aspects and examples for applications of the network model, the main purpose of this paper is to provide the theoretical and physical background. Since the network model is based on the idea of tunneling between magnetic bound states at saddles of the interior potential landscape, a systematic study of this tunneling process will be presented. Also the interesting question, whether or not there is a correspondence between the edge channel picture and the bulk current picture in terms of mixed phases, will also be addressed.

## II. THE SADDLE POINT PROBLEM

The problem of quantized transmission across a saddle-point constriction with magnetic field has been addressed in the past by Büttiker [114]. Büttiker's paper was motivated by the theoretical discussion of quantized conduction steps discovered by van Wees et al [20] and Wharam et al. [21] in split gate constrictions of a 2-dimensional electron gas. Since constrictions in these experiments are electrostatically induced with a pair of split gates, the potential is a smooth function (without hard walls) and the bottleneck of the constriction therefore forms a saddle. At this point our view of the role of potential fluctuations meets the split gate situation referenced above. In this context we look for a link between the results of Büttiker for the bottleneck situation at high magnetic fields and our semi empirical back scattering function  $P(\Delta\nu)$ .

Following the paper of Büttiker for the high magnetic field limit, the trajectories of the states are given by equipotential lines defined by  $\varepsilon = eV(x, y)$ , where  $\varepsilon$  denotes the energy of the guiding center of the classical cyclotron orbit,  $V$  the potential and  $e$  the electron charge. If  $V_0$  denotes the potential of the saddle, the case  $\varepsilon < eV_0$  describes a trajectory, which is repelled by the saddle, where the energy  $\varepsilon$  is finally represented by the Fermi level. Using the considered saddle point as the center of our coordinate system, the minimum distance  $y_n$  between trajectories of the same energy, which are classically repelled on opposite sides to the saddle point, is determined by  $\varepsilon = eV(0, y_n)$  for  $\varepsilon < eV_0$  (see Fig. 3). A similar situation appears for  $\varepsilon > eV_0$ , but turned around by 90 degrees and the minimum distance  $x_n$  is determined by  $\varepsilon = eV(x_n, 0)$ . According to Büttiker, the transmission probabilities in terms of  $x_n$  and  $y_n$  in the high magnetic field limit for the case of  $\varepsilon_n > 0$  is

$$T_{mn} = \delta_{mn} \left\{ 1 + \exp \left[ \pi \frac{\omega_x}{\omega_y} \left( \frac{x_n}{l_B} \right)^2 \right] \right\}^{-1} \quad (2)$$

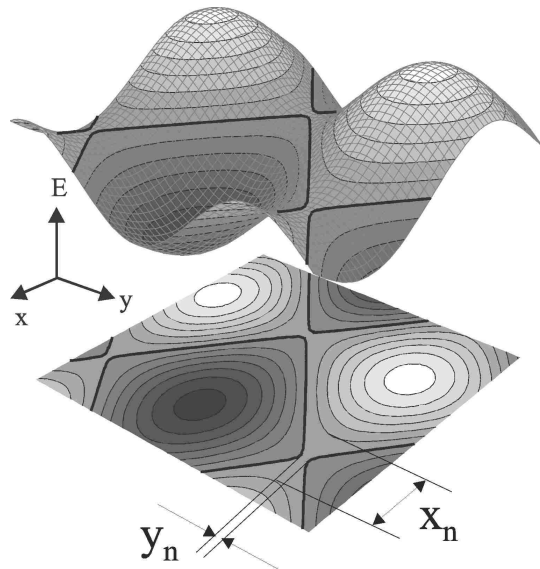


FIG. 3: Example for a two-dimensional potential modulation which forms saddle points. The minimum distances of the closed loops (magnetic bound states) are shown for two different cases:  $y_n$  is achieved, if  $\varepsilon$  is below the saddle energy  $eV_0$  (bold line) and  $x_n$  is achieved, if  $\varepsilon$  is above the saddle energy. All possible loops represent equipotential lines and the selection of the active loops is made by the position of the Fermi level ( $\varepsilon = E_F$ ).

and for the case  $\varepsilon_n < 0$  is

$$T_{mn} = \delta_{mn} \left\{ 1 + \exp \left[ \pi \frac{\omega_y}{\omega_x} \left( \frac{y_n}{l_B} \right)^2 \right] \right\}^{-1} \quad (3)$$

In Eqn.2 and 3 the saddle energy has been defined as zero reference ( $V_0 = 0$ ). The underlying problem is basically a tunneling problem and  $\delta_{nm}$  tells us that this tunneling process with the tunneling rate  $T_{mn}$  happens mainly between the same states (states of same LL) on opposite sides of the saddle. The parameters  $\omega_y$  and  $\omega_x$  result from expanding the potential near the saddle point by

$$V(x, y) \approx V_0 + 0.5m\omega_x^2x^2 - 0.5m\omega_y^2y^2 \quad (4)$$

Now we look for a relation between the transmission rates given above and the function  $P(\Delta\nu)$ , which represents the ration between transmission and reflection  $R/T$  of edge states like used in the network model. If we look for  $x_n$  while  $y_n = 0$  ( $\varepsilon_n = e(V - V_0) > 0$ ), we can easily calculate  $x_n$  from Eqn. 4:

$$x_n^2 = \frac{2\varepsilon_n}{m\omega_x^2} \quad (5)$$

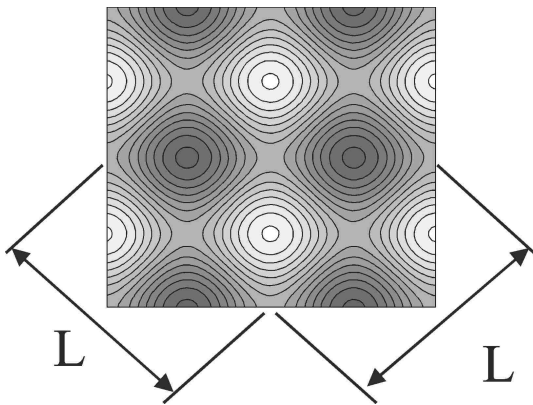


FIG. 4: Contour plot of the artificial 2D Cosine potential. Dark indicates potential minima and the light colored areas indicates the potential maxima.  $L$  is the period of the potential modulation and at the same time it is the grid period of the network.

In the case  $\varepsilon_n < 0$  we get something analogous for  $y_n^2$ :

$$y_n^2 = \frac{2\varepsilon_n}{m\omega_y^2} \quad (6)$$

We introduce an artificial periodic potential modulation, which is a 2-dimensional Cosine - function and which has the same Taylor expansion like Eqn.4:

$$V(x, y) = \tilde{V} [\cos(\omega_y y) - \cos(\omega_x x)] \quad (7)$$

with  $\tilde{V}$  being the potential modulation. Fig. 4 shows a contour plot of the 2-dimensional Cosine potential modulation and we get a saddle point whenever the maximum of the Cosine in one direction meets a minimum of the Cosine in the other direction. In this way we get a periodic array of saddle-points. We consider one saddle to be located exactly at the origin of our coordinate system. If we think about a smoothly varying random fluctuation potential, the average curvature in both directions will be the same. In our representative potential in Eqn. 7 we therefore simplify by setting  $\omega_x = \omega_y = \omega$ , which leads to  $\omega_x/\omega_y = 1$ . In order to re-write Eqn. 2 and Eqn. 3 we do some further substitutions. For the magnetic length  $l_B$  we use:

$$l_B^2 = \frac{h}{2\pi eB} \quad (8)$$

with  $h$  the Plank constant,  $e$  the electron charge and  $B$  the magnetic field. Using further the period length  $L$  of the periodic arrangement of saddle points

$$L = 2\pi/\omega \quad (9)$$

we can rewrite Eqn. 5 and Eqn. 6:

$$x_n^2 = \frac{L^2 \varepsilon_n}{2\pi^2 e \tilde{V}} \quad (10)$$

$$y_n^2 = \frac{L^2 \varepsilon_n}{2\pi^2 e \tilde{V}} \quad (11)$$

Eqn. 8 - 11 now allow to re-write Eqn. 2 and Eqn. 3: Since  $x_n$  and  $y_n$  are described exactly by the same function, but distinguished only by the case  $\varepsilon_n$  either above or below the saddle energy, we can rewrite Eqn. 2 and Eqn. 3 into a single equation as follows:

$$T_{mn} = \delta_{mn} \left\{ 1 + \exp \left[ \pm \frac{L^2 \varepsilon_n eB}{e \tilde{V} h} \right] \right\}^{-1} \quad (12)$$

The signes  $\pm$  indicate the cases  $\varepsilon_n$  above or below the saddle energy. At this point it should be mentioned, that already Haug et al [25] have used a similar equation for addressing the problem of transport across magnetic bound states. They investigated experimentally the effect of a gate electrode across the current path of a QHE sample at constant magnetic field. The major point of that experiment was to study the special situation of having integer filling outside the gate (pure EC transport) and sweeping the gate voltage through non-integer filling below the gate. The authors describe the scattering through the bulk due to the presence of the gate by partly EC back scattering at the gate and partly back scattering via tunneling across magnetic bound states in the gate region. They achieved good agreement with the experiments already by a simplified network consisting of just 2 or 3 magnetic bound states.

In order to be able to compare with the formulation of edge channel back scattering in terms of  $P(\Delta\nu)$ , we have to realize, that the transmission process across the saddle  $T_{mn}$  is formally a back scattering process in the EC picture. Therefore the transmission factor  $T_{mn}$  in Eqn. 12 corresponds to a reflection  $R$  in the edge channel picture. We transform Eqn. 12 into  $P = R/T$  by using  $T_{mn}$  as  $R$  and consequently using  $(1 - T_{mn})$  as  $T$ . :

$$P = \frac{R}{T} = \frac{T_{mn}}{1 - T_{mn}} \quad (13)$$

Since the above tunneling process happens between edge states on opposite side of the saddle but the same Landau level (LL),  $\delta_{mn}$  can be omitted for the further treatment. Further more we have to consider, that the energy  $\varepsilon_n$  is determined by the Fermi level  $E_F$ . In this way we end up with  $P$  as an exponential function of the Fermi level  $E_F$ :

$$P = \exp \left[ \mp \frac{L^2 E_F eB}{e \tilde{V} h} \right] \quad (14)$$

In this equation  $E_F$  is the Fermi level relative to the saddle energy. The ratio  $L^2/\tilde{V}$  can be understood as a measure of the "smoothness" of the potential modulation and  $eB/h$  is the well known number of states in a single LL per unit area. Since  $L$  is the distance between equivalent saddle points,  $L^2$  is the area of the 2-dimensional basis cell of the network grid. It is interesting to note, that the pre-factor of  $E_F$ , which is  $(L^2/e\tilde{V})(eB/h)$ , has the meaning of an average density of states (DOS) in the basis cell of the network, provided that we associate the LL broadening with  $e\tilde{V}$ . In order to consider this aspect in a little more detail, we assume a Gaussian shaped density of states for a single LL [108] and calculate the DOS in the center of the LL as follows:

$$DOS(\varepsilon_n = 0) = \frac{eB}{h} \frac{1}{b\sqrt{\pi}} \quad (15)$$

where  $b$  is the energy broadening of the Gaussian peak. On this background we can calculate the change of the carrier density  $\Delta n$  in a single LL due to the change of  $E_F$  by  $\Delta E_F$  as follows:

$$\Delta n = \frac{eB}{h} \frac{1}{b\sqrt{\pi}} \Delta E_F \quad (16)$$

This is valid for a Fermi level close to the center of the LL, where the DOS is approximately constant. However, we can also represent  $\Delta n$  in terms of the filling factor by  $\Delta\nu = \Delta n/n_{LL}$ , where  $n_{LL} = eB/h$ . This results in:

$$\Delta\nu = \frac{\Delta E_F}{b\sqrt{\pi}} \quad (17)$$

Using again the saddle energy as the zero reference,  $\Delta E_F$  becomes  $E_F$  and  $\Delta\nu$  becomes the difference of the filling factor relative to half filling. Now we can substitute  $E_F$  by  $\Delta\nu$  and rewrite Eqn. 14:

$$P = \exp \left[ -\Delta\nu \frac{b\sqrt{\pi}}{e\tilde{V}} L^2 \frac{eB}{h} \right] \quad (18)$$

Since  $\tilde{V}$  is the amplitude of our artificial potential modulation and  $b$  is the width of the representative DOS - peak, these two parameters correspond to each other. Therefore we can assume, that the pre-factors in the exponent will be a factor of the order of unity, just depending on details of the real potential fluctuations. On this basis we simplify

$$\frac{b\sqrt{\pi}}{e\tilde{V}} \approx 1 \quad (19)$$

and get the following exponential function:

$$P = \exp \left[ -\Delta\nu L^2 \frac{eB}{h} \right] \quad (20)$$

It is easily seen, that the semi-empirical exponential function of Ref. [71] is completely recovered, except the fact, that we get a more complex pre-factor for the filling factor  $\Delta\nu$ . The explicit magnetic field dependence of the pre-factor is a new feature as compared to the earlier semi-empirical function. However, this has no impact on the major features of the function  $P(\Delta\nu)$ , just causing a magnetic field dependence of the width of the plateau transition regimes. If we take a closer look to the exponent, we find  $eB/h$ , which is the number of states per unit area in a LL and  $L^2$ , which is the area of a grid period of the network. As a consequence we get a surprisingly universal result: The exponent of the function  $P(\Delta\nu)$  represents the number of carriers being added ( $\Delta N > 0$ ) or removed ( $\Delta N < 0$ ) from the half filled basis cell of the network grid. This happens if the Fermi level moves away from the center position of the LL.

$$P = \exp[-\Delta N] \quad (21a)$$

$$\Delta N = \Delta\nu L^2 \frac{eB}{h} \quad (21b)$$

This is usually achieved by changing the magnetic field at constant carrier density. However, this change normally happens continuously, meaning that the number of states in a single LL in one grid period is changed just in fractions of unity. This is possible, because in the regime close to a half filled LL there is a strong coupling between the individual grid periods so that the (single) electronic states are well de-localized and can be smeared over several grid periods. A change of the number of electronic states by  $\Delta N = \pm 1$  corresponds to a complete plateau to plateau transition. By considering the grid period length  $L$  as a measure of the smoothness of the potential fluctuations, we get a nice possibility for an interpretation of our result: A large  $L$  corresponds to a rather clean sample (high mobility) with very smooth potential fluctuations and a short  $L$  corresponds to a sample with strong potential fluctuations and hence, strong disorder (low mobility). As a consequence, a large  $L$  indicates a large area of the basis cell of the network and therefore only a small change of the filling factor  $\Delta\nu$  and thus, only a small change of the magnetic field is needed in order to change the number of states by one. This means that we get sharp plateau to plateau transitions on the magnetic field axis. In contrast, a small  $L$ , as expected from samples with strong disorder, leads to a small area of the basis cell, which then requires a large change of the filling factor  $\Delta\nu$  for changing the number of states by the order of one. Therefore we get broad plateau to plateau transitions in this case, exactly what we expect for samples with strong disorder.

On the basis of geometric arguments and using a checkerboard as representative for the network (Fig. 5) Eqn. 21 allows also another simple interpretation: Using directly the trajectories of the channels at different

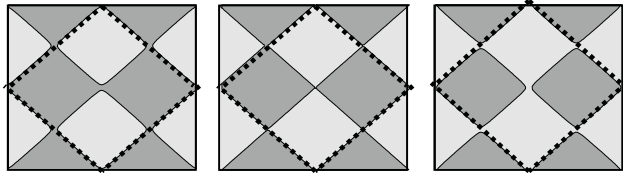


FIG. 5: Spatial distribution of filled (dark colored) and empty (light colored) states for left:  $E_F > E_{LL}$ , middle:  $E_F = E_{LL}$  and right:  $E_F < E_{LL}$ . The dotted line indicates the basis cell of the network.

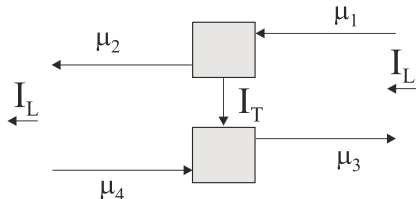


FIG. 6: Schematic representation of the effect of back scattering in the EC-picture.

Fermi levels we get 3 cases as shown in Fig. 5: (i) if the Fermi level is above the saddle energy (center of LL), the filled states dominate the transport properties, because they build an interconnected network. (ii) if the Fermi level coincides with the saddle energy, filled and empty states take up exactly half of the space, which also means exactly a half filled LL. (iii) if  $E_F$  is below the saddle energy, the empty states (insulating phase) build an interconnected network, leaving isolated droplets of filled states and leading to a high resistive regime. It should be mentioned, that already Mashida et al. used such a picture for the interpretation of their experimental results[51, 94].

### III. DISCUSSION

By using a representative 2-dimensional Cosine potential modulation, a result by Büttiker [114] for the saddle point problem at high magnetic fields was transformed into the back scattering function  $P(\Delta\nu)$ , which is used for the nodes of the network according to Ref. [85]. One main extension as compared to Ref. [114] is the treatment of the tunneling current within the framework of the Landauer-Büttiker formalism. This means that a transverse current between a channel pair (tunneling current serves as a back scattering current between channels), leads to a longitudinal potential drop in each of the channels. This can be considered as the essence of the EC-picture within the LB-formulation and there is no classical way to account for this behavior. In order to point out this fact somewhat more clearly, the situation is sketched in Fig. 6.

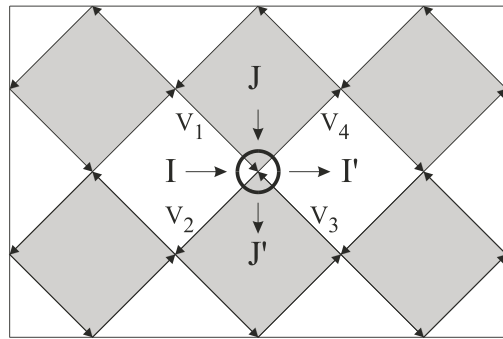


FIG. 7: Checkerboard model for bulk current transport in the QHE regime after Ruzin et al [12]. The dark and light areas represent different quantum Hall liquids with different Hall conductance. Currents  $I$  and  $J$  are assumed to flow exclusively in the corresponding phase and the total behavior of the conductor is determined by the mixture of both phases.

If there is a longitudinal current  $I_L$ , it is carried dissipation-less by a channel pair and is represented on the right side by  $I_L = (\mu_1 - \mu_3)e^2/h$  and on the left side by  $I_L = (\mu_2 - \mu_4)e^2/h$ , while  $(\mu_1 - \mu_3) = (\mu_2 - \mu_4)$  for current conservation reasons. A transverse current  $I_T$ , which may be enabled by some conduction or tunneling between opposite channels causes a longitudinal voltage drop. This is because  $I_T$  has to be represented also within the LB formalism according to  $I_T = (\mu_1 - \mu_2)e^2/h$  on the upper edge and  $I_T = (\mu_3 - \mu_4)e^2/h$  at the lower edge, while  $(\mu_1 - \mu_2) = (\mu_3 - \mu_4) = \Delta\mu_L$ , again because of current conservation reasons. It is important to note, that any current ( $I_L$  or  $I_T$ ) within the EC-picture is defined only by a pair of directed channels, which must not be confused with a difference of opposite directed classical currents. As a consequence, it is not possible to assign a current to any single directed channel and the occurrence of a perpendicular current  $I_T$  does not change the longitudinal current  $I_L$ . This is a fact, which must not be misinterpreted as a violation of Kirchhoff's law of current conservation. Using finally the ration  $I_T/I_L$  as an equivalent for  $R/T$  of the LB formalism, it is easily shown that the longitudinal voltage drop  $\Delta\mu_L$  is coupled to the Hall voltage like  $\Delta\mu_L = (\mu_1 - \mu_2) = (\mu_1 - \mu_3)R/T$ , with  $R/T$  identified as  $P$ , which is the function derived in this paper.

The above summarized view of the EC-picture has been used already in Ref. [60] in order to explain an anomalous behavior of the magneto transport of high mobility quasi 3-dimensional PbTe wide quantum wells. Also in Ref. [71] this interpretation of the EC-picture has been successfully used which finally led to the application within the discussed network model. From this point of view the network model can be considered to be based purely on the EC-picture and the LB-formalism. It is therefore quite surprising, that also the ohmic regime is quite well represented. However, this puzzle can be resolved by reconsidering Fig. 5, which appears like a checker board representation of the network. From this

point of view it meets the approach of Ruzin et al [12]. Ruzin et al used such a checker board model for bulk transport in the QHE regime in order to obtain a universal relation between longitudinal and transverse conductances in the QHE and Fig.5 summarizes this concept: Ruzin et al considered two competing quantum Hall liquids in the presence of a long-range random potential, with the magnetic field determining the area fractions close to 1/2. Fig. 7 represents this situation for an artificial periodic long-range potential. The "white" regions represent the phase with quantized Hall conductance  $\sigma_1$ , and the "dark" regions those of Hall conductance  $\sigma_2$ . If the situation is such that the "white" phase percolates freely throughout the sample, the system will be on the plateau with  $\sigma_{xy} = \sigma_1$ . Similarly if the "dark" regions percolate freely, the system will be on the plateau with  $\sigma_{xy} = \sigma_2$ . Near the percolation threshold transport is controlled by quantum tunneling between clusters of the same phase at the saddle points. Ruzin et al related the net currents in the four quadrants to the four electric potentials at the edges  $V_1$  through  $V_4$  as given by:

$$I = \sigma_1(V_2 - V_1) \quad (22a)$$

$$J = \sigma_2(V_3 - V_2) \quad (22b)$$

$$I' = \sigma_1(V_3 - V_4) \quad (22c)$$

$$J' = \sigma_2(V_4 - V_1) \quad (22d)$$

Postulating current conservation within the individual phases ( $I = I'$  and  $J = J'$ ), Ruzin et al get automatically  $(V_2 - V_1) = (V_3 - V_4)$ , which is identical to the results of our treatment as illustrated in Fig. 6. Further on, Ruzin et al obtained a universal semi-circle-relation between longitudinal and transverse conductance. At this point it should be mentioned, that such a semicircle relation has also been obtained within our preceding work [68, 71], which once more demonstrates the agreement of our results with the results of Ruzin et al. However, our model achieves additional results such as the filling factor dependence and transport parameters in terms of  $R_{xx}$  and  $R_{xy}$  as well as the distribution of the applied voltage across the sample area. There is also a qualitative difference between Ruzin's and our picture: In our picture the space is divided between occupied and non-occupied states, while Ruzin et al are talking about 2 competing quantum Hall liquids (QHL) of different Hall conductivity. We can overcome this disagreement by recognizing, that in our model each involved LL is represented by a separate network with its own mixture of empty and filled states, which we associate with the insulator and a QHL phase of Hall conductance  $\sigma = e^2/h$  respectively.

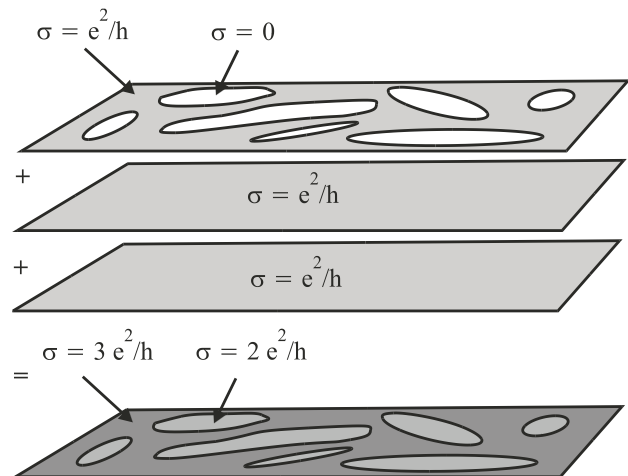


FIG. 8: Scheme for combining individual LLs, where each of them may have a mixture of quantum Hall liquid and insulating phase. In this case it is assumed that just the top LL is partly occupied and all lower ones are completely filled. The result is a combined system of mixed phases of different quantum Hall liquids, which means different Hall conductivities.

In the case of the IQHE there is always just one partly filled (top) LL and all lower ones are completely filled. For each LL the QHL phase exhibits a quantized Hall conductance of  $\sigma = e^2/h$ , while the Hall conductance for the insulator phase  $\sigma = 0$ . For the complete system in the bulk current representation we have to sum up all contributions of all LLs locally, which leads to a situation like sketched schematically in Fig. 8. Putting forward a bulk current representation, one has to add all Hall conductivities of all involved LLs locally and the resulting picture becomes again similar to that one of Ruzin et al. At this point we want to make clear, that at this stage our network model does not include non-linear effects, which means that it considers the electron system to be sufficiently close to thermal equilibrium. However, for thermal equilibrium some similarity between bulk and edge current picture might not be that surprising. A recent theoretical treatment of non-linear transport through mesoscopic systems by Sanchez et al [103] shows a possible magnetic field asymmetry, which is not within the scope of our network model in the present state of development. Nevertheless it is possible to describe selective current injection into edge stripes also within our network model, like e.g. achieved by selective EC reflection due to gate electrodes[85], while we cannot see how this could be achieved within the bulk current picture. Another important aspect to be mentioned at this point is that in our network the phase coherence is not maintained over more than one single grid period, but still exact quantization of the QHE is obtained. This is in agreement with theoretical results of F. Gagel et al [55] who found a surprising stability of the QH plateaus against dissipation and phase destroying events.

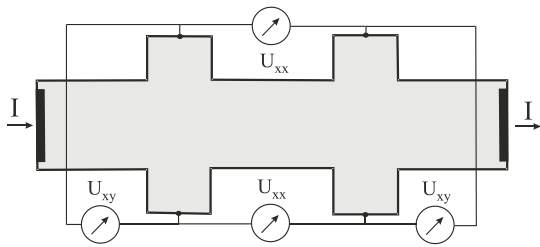


FIG. 9: Sample layout as used for the numerical Simulations.

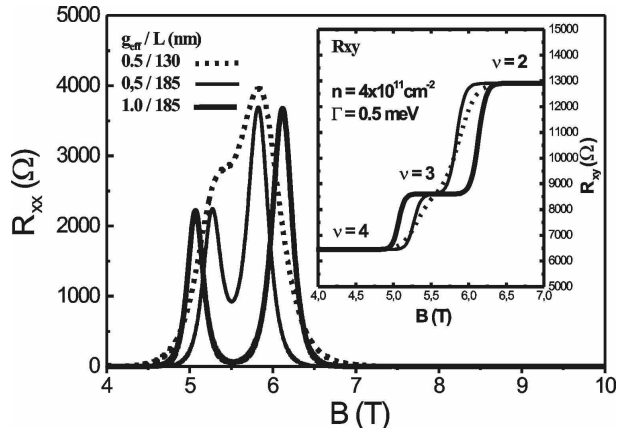


FIG. 10: Results for magneto transport data in the high field regime calculated with Eqn. 20 as the coupling function for the nodes of the network. The calculation is done for 2 different effective  $g$ -factors ( $g_{eff} = 0, 5$  and  $g_{eff} = 1.0$ ) and two different values for  $L = 130nm$  and  $L = 185nm$ .

#### IV. SIMULATION RESULTS

If we use Eqn. 20 as a replacement of the original function of Ref. [85], we get results for the magneto transport simulation as shown in Fig. 10 and Fig. 11. The layout of the sample is shown in Fig. 9. Considering the individual plateau transitions at high magnetic fields, there is no qualitative difference to the results of the previous version. The major difference and improvement concerns the low magnetic field range. At very low magnetic fields the zeros in  $R_{xx}$  disappear and the Hall effect starts as a straight line, and turns gradually over to a plateau behavior at higher fields. The reason for this is the explicit magnetic field dependence of the exponent in Eqn. 20, which leads to wide plateau transitions at low magnetic fields and sharp plateau transitions at high magnetic fields. This results in an overlap of the ohmic (dissipative) regimes of several LLs at low fields. In order to get the individual filling factors in case of LL overlap, the individual spin split LLs have been calculated using the standard parameters for GaAs and a LL broadening according to  $\Gamma = \Gamma_0\sqrt{B}$  [108] has been used by setting  $\Gamma_0 = 0.5meV$ .

The actual calculation consists of two main parts: (I) For calculating the occupation numbers standard procedures are used and the Fermi level in the bulk region

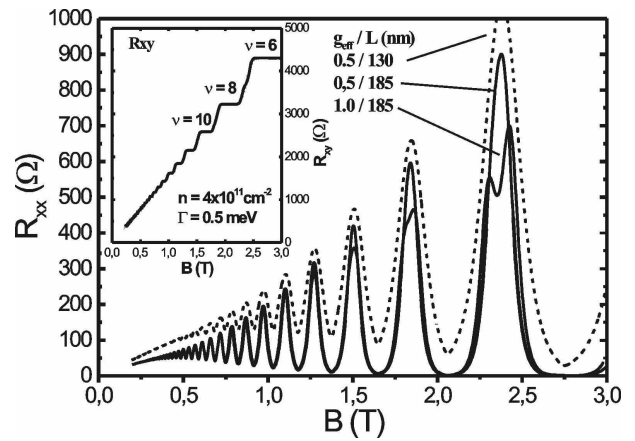


FIG. 11: Results for magneto transport data in the low field regime calculated with Eqn. 20 as the coupling function for the nodes of the network. The calculation is done for 2 different effective  $g$ -factors ( $g_{eff} = 0, 5$  and  $g_{eff} = 1.0$ ) and two different values for  $L = 130nm$  and  $L = 185nm$ .

is calculated by filling up the density of states (DOS) with the constant bulk carrier density. The DOS is composed by the superposition of the magnetic field dependent Gaussian shaped DOS of spin split LLs. The Fermi level for regions of non-zero electrostatic bare potential (edges and gate regions) is forced to match the obtained (magnetic field dependent) Fermi level in the bulk. This allows to get a self-consistent electrostatic potential and a rearrangement of the carrier density at the edges, which results in an electrostatic edge potential according to Chlovskii et al [2]. (II)The such obtained lateral carrier density profile is transferred to the nodes of the network and in another self-consistent iteration procedure the lateral distribution of the bias voltage, which is introduced via the current contacts, is calculated. From this the potential difference for any designated pair of voltage probes is obtained as a function of the magnetic field. A metallic contact is realized by interconnecting all channels of all involved LLs at the position of the designated contact point[85]. Extended metallic contacts are realized by creating arrays of such contact points. The current at the current contacts is calculated only after arriving at the self-consistent solution in the network, which allows finally to calculate the various resistances. This means, that in principle a constant supply voltage is used in the network model instead of a constant supply current like in most experiments. However, for calculating the resistances for a standard QHE setup with a single current source this makes no difference. For achieving a constant current mode, the potentials at the current contacts are additionally varied in a proper way during the iteration procedure in order to get the required pre-set current. In this way a one-to-one simulation of experiments using constant supply currents and measuring voltages at several potential probes is possible.

Just for demonstration, the influence of spin splitting by using different effective  $g$ -factors such as  $g^* = 0.5$  and



$g^* = 1.0$  and different values for  $L$ , such as  $L = 135\text{nm}$  and  $L = 185\text{nm}$ , is simulated. The results are shown in Fig. 10 for the high magnetic field range and in Fig. 11 for low magnetic fields. For  $L = 135\text{nm}$  and  $g^* = 0.5$  spin splitting is hardly to observe even at high fields around 5 Tesla, while for the case  $L = 185\text{nm}$  a well resolved spin splitting can be observed even for a small g-factor of  $g^* = 0.5$ . At magnetic fields around 2.5 Tesla spin splitting is only weakly pronounced even for  $g^* = 1$  and  $L = 185\text{nm}$ . In summary one can say, that this overall behavior looks quite realistic and a more systematic study on the possibility of a more accurate determination of an enhanced effective g-factor from transport data is planned separately.

## V. SUMMARY

Starting with a treatment of the saddle point problem in the high magnetic field limit by Büttiker we have been able to show, that it is possible to transform Büttikers re-

sults into a filling factor dependent back scattering function  $P(\Delta\nu)$ . This function is used as the coupling function for the nodes of a recently developed new network model for the QHE regime of 2D systems. As a result, the numerical simulation based on this network delivers transport data, in which  $R_{xy}$  starts with a classical straight line while  $R_{xx}$  shows no zeros. With increasing magnetic field the IQHE sets-in with Shubnikov-de Haas oscillations in  $R_{xx}$ , followed by zeros in  $R_{xx}$  and plateaus in  $R_{xy}$ , like seen in experimental data. For equilibrium conditions we have found an equivalence between the bulk current picture in terms of mixed phases like used by Ruzin et al and our network representation on the basis of the Landauer-Büttiker formalism.

## VI. ACKNOWLEDGEMENTS

The author thanks M. Büttiker for stimulating discussions and comments.

- 
- [1] M. Büttiker, Phys. Rev. B38, 9375 (1988)
  - [2] D.B. Chlovskii, B.I. Shklovskii, L.I. Glatzman, Phys.Rev. B46, 4026 (1992)
  - [3] H. Hirai, S. Komiyama, Jpn. J. Appl. Phys. 34, 4321 (1995)
  - [4] T. Christen, M. Büttiker, Phys. Rev. B53, 2064 (1996)
  - [5] H.P. Wei, D.C. Tsui, M.A. Paalanen, A.M.M. Pruiskien, Phys.Rev.Lett 61, 1294 (1988)
  - [6] S. Koch, R.J. Haug, K.v. Klitzing, K. Ploog, Phys. Rev. Lett 67,883 (1991)
  - [7] S. Koch, R.J. Haug, K.v. Klitzing, K. Ploog, Phys. Rev. B 46, 1596 (1992)
  - [8] H.P. Wei, L.W. Engel, D.C. Tsui, Phys. Rev. B50, 14609 (1994)
  - [9] F.Hohls, U.Zeitler, R.J.Haug, R.Meisels, K.Dybko, F.Kuchar Phys.Rev.Lett. 89, 2768011-2768014 (2002)
  - [10] B. Huckestein, Rev. Mod. Phys. 67 (1995) 357
  - [11] S.L. Sondhy, S.M. Girvin, J.P. Carini, D. Shahar, Rev. Mod. Phys. 69, 315 (1997)
  - [12] I. Ruzin and S. Feng, Phys Rev, Lett 74, 154 (1995)
  - [13] K.v. Klitzing, G. Dorda, M. Pepper, Phys. Rev. Lett. 45, 494 (1980)
  - [14] F.F. Fang, P.J. Stiles, Phys. Rev. B27, 6497 (1983)
  - [15] F.F. Fang, P.J. Stiles, Phys. Rev. B 29, 3749 (1984)
  - [16] B.E. Kane, D.C. Tsui, G. Weimann, Phys. Rev. Lett. 59, 1353 (1987)
  - [17] P. Streda, J. Kucera, A.H. MacDonald, Phys. Rev. Lett 59, 1973 (1987)
  - [18] H.A. Fertig and B.I. Halperin, Phys. Rev. B 36, 7969 (1987)
  - [19] J.K. Jain, S.A. Kivelson, Phys. rev. Lett 60, 1542 (1988)
  - [20] B.J. van Wees et al., Phys. Rev. Lett 60, 848 (1988)
  - [21] A. Wharam et al., J. Phys. C 21, L209 (1988)
  - [22] S. Komiyama, H. Hirai, S. Sasa, S. Hiyamizu, Phys. Rev. B 40, 12566 (1989)
  - [23] B.J. van Wees, E.M.M. Willems, C.J.P.M. Harmans, C.W.J. Beenakker, H. van Houten, J.G. Williamson, C.T. Foxon, J.J. Harris, Phys. Rev. Lett 62, 1181 (1989)
  - [24] B.J. van Wees, L.P. Kouwenhoven, C.J.P.M. Harmans, J.G. Williamson, C.E. Timmering, M.E.I. Broekaart, C.T. Foxon, J.J. Harris, Phys. Rev. Lett 62, 2523 (1989)
  - [25] R.J. Haug, J. Kucera, P. Streda, K. von Klitzing, Phys. Rev. B 39, 10892 (1989)
  - [26] B.W. Alphenaar, P.L. McEuen, R.G. Wheeler, R.N. Sacks, Phys. Rev. Lett. 64, 677 (1990)
  - [27] , T. Martin, S. Feng, Phys. rev. Lett 64, 1971 (1990)
  - [28] G. Müller, D. Weiss, S. Koch, K. v. Klitzing, H. Nickel, W. Schlapp, R. Lösch, Phys. Rev. B 42, 7633 (1990)
  - [29] A.K. Geim, P.C. Main, P.H. Beton, P. Streda, L. Eaves, C.D.W. Wilkinson, S.P. Beaumont, Phys. Rev. Lett. 67, 3014 (1991)
  - [30] J.A. Simmons, S.W. Hwang, D.C. Tsui, H.P. Wei, L.W. Engel, M. Shayegan, Phys. Rev. B 44, 12933 (1991)
  - [31] C.J.B. Ford, S. Washburn, R. Newbury, C.M. Knoedler, J.M. Hong, Phys. Rev. B 43, 7339 (1991)
  - [32] P.C. van Son, F.W. de Vries, T.M. Klapwijk, Phys. Rev. B 43, 6764 (1991)
  - [33] H. Nii, M. Ohsawa, S. Komiyama, S. Fukatsu, Y. Shiraki, R. Itoh, H. Toyoshima, Surface Science 263, 275 (1992)
  - [34] S. Komiyama, H. Hirai, M. Ohsawa, Y. Matsuda, S. Sasa, T. Fujii, Phys. Rev. B 45, 11085 (1992)
  - [35] B.W. Alphenaar, A.A.M. Staring, H. van Houten, M.A.A. Mabesoone, C.T. Foxon, Phys. Rev. B 46, 7236 (1992)
  - [36] S. Komiyama, H. Hirai, M. Ohsawa, Y. Matsuda, S. Sasa, T. Fujii, Phys. rev. B 45, 11085 (1992)
  - [37] R. Merz, F. Keilmann, R.J. Haug, K. Ploog, Phys. Rev. Lett. 70, 651 (1993)
  - [38] D.L. Maslov, D. Loss, Phys. Rev. Lett. 71, 4222 (1993)
  - [39] D.H. Lee, Z. Wang, S. Kivelson, Phys. Rev. Lett 26, 4130 (1993)

- [40] J.E. Müller, Phys. Rev. Lett. 72, 2616 (1994)
- [41] P.C. Main, A.K. Geim, H.A. Carmona, C.V. Brown, T.J. Foster, R. Taboryski, P.E. Lindelof, Phys. Rev. B 50, 4450 (1994)
- [42] H. Hirai, S. Komiyama, Phys. rev. B 49, 14012 (1994)
- [43] A.J. Peck, S.J. Bending, J. Weis, R.J. Haug, K.v. Klitzing, K. Ploog, Phys. Rev. B 51, 4711 (1995)
- [44] K. Oto, S. Takaoka, K. Murase, Jpn. J. Appl. Phys. 34, 4332 (1995)
- [45] R. Schuster, K.Ensslin, V. Dolgoplov, J.P. Kotthaus, Phys. Rev. B 52, 14699 (1995)
- [46] A. Kristensen, C.J. Kennedy, P.E. Lindelof, M. Persson, Semicond. Sci. Technol. 10, 1315 (1995)
- [47] B.J. van Wees, G.I. Meijer, J.J. Kuipers, T.M. Klapwijk, W. van de Graaf, G. Borghs, Phys. Rev. B 51, 7973 (1995)
- [48] R.J.F. van Haren, W. de Lange, F.A.P. Blom, J.H. Wolter, Phys. Rev. B 52, 5760 (1995)
- [49] I.V. Zozulenko, F.A. Maa, E.H. Hauge, Phys. Rev. B 51, 7058 (1995)
- [50] B.L. Johnson, A.S. Sachrajda, G. Kirzenow, Y. Feng, R.P. Taylor, L. Henning, J. Wang, P. Zawadzki, P.T. Colderidge, Phys. Rev. B 51, 7650 (1995)
- [51] T. Mashida, H. Hirai, S. Komiyama, Y. Shiraki, Phys.Rev. B54, 16860 (1996)
- [52] E. Yahel, D. Orgad, A. Palevski, H. Shtrikman, Phys. Rev. Lett 76, 2149 (1996)
- [53] M. Rahman, J.H. Davies, I.A. Larkin, M.C. Holland, A.R. Long, J.G. Williamson, Phys. Rev. B 54, 16409 (1996)
- [54] R.G. Mani, Journal Phys. Soc. Japan, 1751 (1996)
- [55] F. Gagel, K. Maschke, Phys. Rev. B 54, 13885 (1996)
- [56] J.Oswald, G. Heigl, M. Pippan, G. Span, T. Stellberger, D.K.Maude, J.C.Portal, Surface Science 361/362, 525 (1996)
- [57] J.Oswald, G.Heigl, G.Span, A.Homer, P.Ganitzer, D.K.Maude, J.C.Portal, Physica B 227, 360 (1996)
- [58] Y.-C. Kao, D.-H. Lee, Phys. Rev. B 54, 16903 (1996)
- [59] T.Mashida, H.Hirai, S.Komiyama, Solid State Commun. 103, 441 (1997)
- [60] J.Oswald, G. Span, Semicond. Sci. Technol. 12, (1997) 345
- [61] J.P. Bird, M. Stopa, K. Connolly, D.P. Pivin, Jr., D.K. Ferry, Y. Aoyagi, T. Sugano, Phys. Rev. B 56, 7477 (1997)
- [62] D. Shahar, D.C. Tsui, M. Shayegan, E. Shimshoni, S.L. Sondhi, Phys. Rev. Lett. 79, 479 (1997)
- [63] K. Tsemekhman, V. Tsemekhman, C. Wexler, D.J. Thouless, Solid State Commun. 101, 549 (1997)
- [64] R.G. Mani, Appl. Phys. Lett. 70, 2879 (1997)
- [65] J.Oswald, G. Heigl, G. Span, A. Homer, P. Ganitzer, D.K.Maude, J.C.Portal, Proc.of 12th Int. Conf. on the Appl. of High Magnetic Fields, Wrzburg 1996, Vol 1, 227, World Scientific, Singapore (1997)
- [66] J.Oswald, G. Span, A. Homer, G. Heigl, P. Ganitzer, D.K. Maude, J.C. Portal, Solid State Commun. 102, 391 (1997)
- [67] D. Shahar et al, Solid State Commun. 102 (12)(1997) 817
- [68] J. Oswald, G. Span, F. Kuchar, Phys. Rev. B 58 (1998) 15401
- [69] T. Mashida, H.Hirai, S. Komiyama, Y. Shiraki, Physica B 249-251, 128 (1998)
- [70] A. Furusaki, Physica B 249-251, 430 (1998)
- [71] J. Oswald, Physica E 3 (1998) 30
- [72] T.Mashida, H. Hirai, S.Komiyama, Y. Shiraki, Solid-State Electron. 42, 1155 (1998)
- [73] J.Oswald, G.Span, A.Homer, G.Heigl, P.Ganitzer, D.K.Maude, J.C.Portal, Proc. of the 8th Int. Conf. On Narrow Gap Semiconductors, Shanghai 1997, World Scientific, 304-307 (1998)
- [74] J.Oswald, G.Span, A.Homer, G.Heigl, P.Ganitzer, D.K.Maude, J.C.Portal, Proc. of the 8th Int. Conf. on Narrow Gap Semiconductors, Shanghai 1997, World Scientific, 300-303 (1998)
- [75] P.Ganitzer, A.Homer, M.Lucyshyn, B.Jamnik, J.Oswald, D.K.Maude J.C. Portal, Physica B 256-258, 600-603 (1998)
- [76] A.Homer, P.Ganitzer, G.Span, J.Oswald, Superlattices and Microstruct. 25, 191 (1999)
- [77] J. Oswald, A. Homer, P. Ganitzer, Microelectron. Eng. 47 (1999) 31
- [78] T. Heinzel, Y. Acremann, K. Ensslin, E. Gini, H. Melchior, M. Holland, Physica E7(3-4), 804 (2000)
- [79] T. Mashida, S. Ishizuka, K. Muraki, Y.Hirayama, S. Komiyama, Physica E 6, 152 (2000)
- [80] M.T. Woodside, C. Vale, P.L. McEuen, C. Kadow, K.D. Maranowski, A.C. Gossard, Phys.Rev. B 64 (4), 041310/1-4 (2001)
- [81] H. Fujioka, S. Katsumoto, Y. Iye, Jap. J. Appl. Phys. 40(3B), 2073 (2001)
- [82] K. Arai, K. Oto, S. Takaoka, K. Murase, Physica E. 9(2). 243 (2001)
- [83] E. Ahlswede, P.Weitz, J. Weis, K. von-Klitzing, K. Eberl, Physica B 298(1-4), 562 (2001)
- [84] T. Mashida, S. Ishizuka, S. Komiyama, Koji Muraki, Y. Hirayama, Phys.Rev B63, 045318 (2001)
- [85] J. Oswald, A. Homer, Physica E 11, 310 (2001)
- [86] J. Oswald, Proc. 25th Int. Conf. on the Physics of Semiconductors in Osaka 2000, Springer Proceedings in Physics 87, 977 (2001).
- [87] T. Machida, S.Ishizuka, T. Yamazaki, S. Komiyama, K. Muraki, Y. Hirayama, Phys. Rev. B 65(23), 233304 (2002)
- [88] E. Ahlswede, J. Weis, K. von-Klitzing, K. Eberl, Physica E 12(1-4), 165 (2002)
- [89] A. Wurtz, R. Wildfeuer, A. Lorke, E.V. Deviatov, V.T. Dolgoplov, Phys.Rev.B 65, 075303(2002)
- [90] J.Oswald, 15th Int. Conf. on High Magnetic Fields in Semiconductor Physics, SEMIMAG, 5-9 Aug, 2002, Oxford, U.K., CD-ROM
- [91] J. Oswald, Y. Ochiai, N.Aoki, L.-H. Lin, K. Ishibashi, Y. Aoyagi, Microelectronic Engineering 63, 91 (2002)
- [92] K. Ensslin, Superlattice and Microstruct 33, 425 (2003)
- [93] S. Komiyama O. Astafiev T. Machida, Physica E 20, 43 (2003)
- [94] Y. Kawano, S. Komiyama, Phys. Rev. B 68, 085328 (2003)
- [95] M. Blaauboer, Phys. Rev. B 68 (20), 205316 (2003)
- [96] K. Takashina, R.J. Nicholas, B. Kardynal, N.J. Mason, D.K. Maude, J.C. Portal, Phys Rev B 68 (23), 235303 (2003)
- [97] M. Büttiker, P. Samuelsson, E.V. Sukhorukov, Physica E 20, 33 (2003)
- [98] E. Peled, D. Shahar, Y. Chen, E. Diez, D.L. Sivco, A.Y. Cho, Phys Rev Lett 91(23), 236802 (2003)
- [99] T. Machida, T. Yamazaki, K. Ikushima, S. Komiyama, Appl. Phys. Lett 82(3), 409 (2003)

- [100] Y.Kawano, S. Komiyama, Phys. Rev. B 68(08), 085328 (2003)
- [101] K. Arai, S. Hashimoto, K. Oto, K. Murase, Phys. Rev. B 68, 165347 (2003)
- [102] A. Cresti, G. Grosso, G.P. Parravicini, Phys. Rev. B 69(23), 233313 (2004)
- [103] David Sanchez and Markus Büttiker, Phys. Rev. Lett. 93, 106802 (2004)
- [104] P. Samuelsson, E.V. Sukhorukov, M. Büttiker, Phys. Rev. Lett. 92(2), 026805 (2004)
- [105] E. Peled, Y. Chen, E. Diez, D.C. Tsui, D. Shahar, D.L. Sivco, A.Y. Cho, Phys Rev B 69, 241305(R) (2004)
- [106] F.W. Hehl, Y.N. Obukhov, B. Rosenow, Phys Rev Lett 93(9), 096804 (2004)
- [107] E.V. Deviatov, A. Wurtz, A. Lorke, M.Yu.Melnikov, V.T. Dolgoplov, D. Reuter, A.D. Wieck, Phys Rev B 69(11), 115330 (2004)
- [108] M.Russ, A. Lorke, D.Reuter, P.Schafmeister, Physica E22, 506 (2004)
- [109] Y. Seo, B. Eom, I. Yu, K. Park, S. Lee, Solid State Commun 130(6), 391 (2004)
- [110] S. Kicin, T. Pioda, T. Ihn, K. Ensslin, D.D. Driscoll, A.C. Gossard, Physica E 21, 708, (2004)
- [111] R. Landauer, IBM J.Res.Dev. 1, 223 (1957)
- [112] M. Büttiker, Y. Imry, R. Landauer, S. Pinhas, Phys. Rev. B 31, 6207 (1985)
- [113] J.T.Chalker, P.D.Coddington, J.Phys. C 21 (1988) 2665.
- [114] M. Büttiker, Phys. Rev. B 41, 7906 (1990)
- [115] S. Cho, M.P.A. Fisher, Phys. Rev. B 55, 1637 (1997)
- [116] D.P. Arovas, M. Janssen, B. Shapiro, Phys. Rev. B 56, 4751 (1997)
- [117] P. Cain, R.A. Römer, M. Schreiber, M.E. Raikh, Phys. Rev. B 64, 235326 (2001)